TITLE

Targeted Elimination of Mutated Mitochondrial DNA by a Multi-functional Conjugate Capable of Sequence-specific Adenine Alkylation

AUTHORS

Takuya Hidaka,[1] Kaori Hashiya,[1] Toshikazu Bando,[1] Ganesh N. Pandian,[2,*] and Hiroshi Sugiyama[1,2,*]

[1] Department of Chemistry, Graduate School of Science, Kyoto University, Sakyo, Kyoto 606-8501, Japan

[2] Institute for Integrated Cell-Material Science (WPI-iCeMS), Kyoto University, Sakyo, Kyoto 606-8501, Japan.

Correspondence: namasivayam.ganeshpandian.5z@kyoto-u.ac.jp; hs@kuchem.kyoto-u.ac.jp

GRAPHICAL ABSTRACT

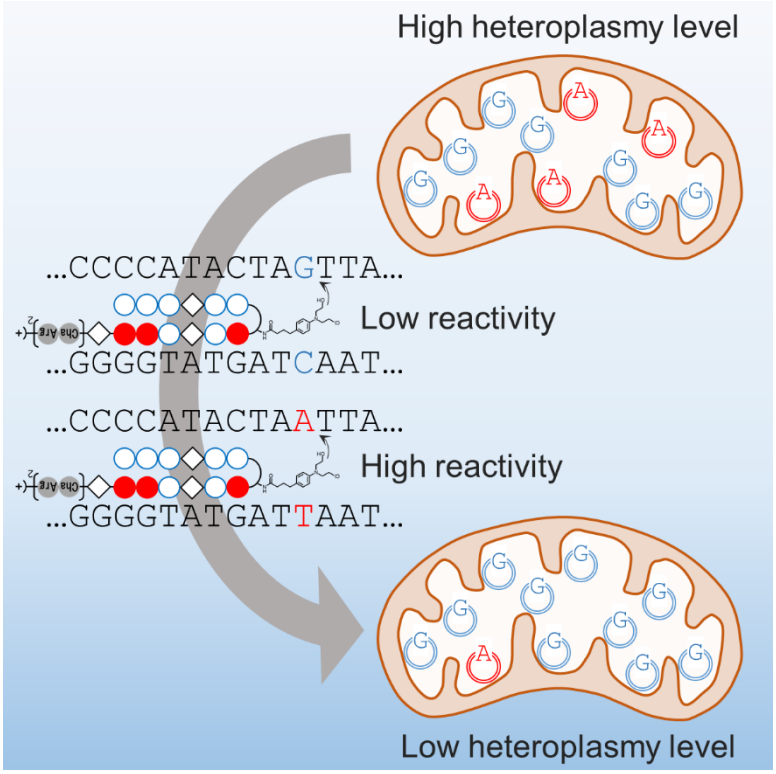

SUMMARY

Mutations in mitochondrial DNA (mtDNA) cause mitochondrial diseases, characterized by abnormal mitochondrial function. Although eliminating mutated mtDNA could cure mitochondrial diseases and has been demonstrated using mitochondria-directed nucleases, no chemical-based drugs in clinical trials are capable of selective modulation of mtDNA mutations. Here, we constructed a new class of compounds encompassing pyrrole-imidazole polyamides (PIPs) as sequence-selective DNA binding domains, mitochondria-penetrating peptide for mitochondrial delivery and chlorambucil, a DNA-alkylating reagent with the adenine-specific reactivity. *In vitro* DNA alkylation assay showed that our compound "**8950A-Chb(Cl/OH)**" targeting a non-pathogenic point mutation in HeLa S3 cells (m.8950G>A) could specifically alkylate the mutant adenine and reduce the mtDNA possessing the target mutation in cultured HeLa S3 cells. The programmability of PIPs to target different sequences could allow this new class of compounds to be developed as designer drugs targeting pathogenic mutations associated with mitochondrial diseases in future studies.

INTRODUCTION

Mitochondria are ubiquitous cellular organelles with a fundamental role in cellular metabolism functions like energy production, cellular homeostasis, biosynthesis of biomolecules, and metabolic waste management (Spinelli and Haigis, 2018). They also play a pivotal role in other cellular processes, including calcium homeostasis, nonshivering thermogenesis, and apoptosis (Hopper et al., 2006; Hughes et al., 2009; Rasola and Bernardi, 2011; Rizzuto et al., 2012). Proteomic analyses have found that mitochondrial function is maintained by about 1500 proteins (approximately 10% of the cellular proteome), while some mitochondrial genes are encoded by mitochondrial DNA (mtDNA). Human mtDNA encodes 37 genes including 13 protein-coding genes required for the electron transport chain, 22 tRNA, and two rRNA. Individual cells contain multiple copies of mtDNA, with 200–2000 copies in each somatic cell (Robin and Wong, 1988).

Mitochondrial diseases are inherited disorders characterized by deficiencies in mitochondrial function caused by mutations in nuclear DNA (nDNA) and mtDNA (Gorman et al., 2016). The first two mtDNA mutations were identified in 1988: i.e., deletions in mitochondrial myopathies and a point mutation in the *MT-ND4* gene (m. 11778A>G) causing Leber's hereditary optic neuropathy (Douglas C. Wallace et al., 1988; Holt et al., 1988). To date, over 800 point mutations in mtDNA have been registered in the human mitochondrial genome database, MITOMAP (Kogelnik et al., 1996). The presence of multiple copies of mtDNA can lead to a mixture of mutant and wild-type mtDNA in individual cells, a state known as heteroplasmy. Although mitochondrial function can be maintained by

residual wild-type mtDNA when the heteroplasmy level is low, a high proportion of mutant mtDNA exceeding a critical threshold level impairs mitochondrial function (threshold effect) (Boulet et al., 1992). To cure mitochondrial diseases, mutant mtDNA should be removed from all cells. The current approach to achieve this complex task is to use mitochondria-directed nucleases, such as restriction enzyme (Bayona-Bafaluy et al., 2005), zinc finger nucleases (mtZFNs) (Gammage et al., 2014 and 2018), and transcription activator-like effector nucleases (mito-TALENs) (Bacman et al., 2013 and 2018), which are programmed to selectively digest the mutant sequence (Jackson et al., 2020). Although these approaches display promise with regard to gene therapies, problems related to possible genomic alterations by expression vectors and the use of viral vectors are major barriers to clinical application.

Chemical-based approaches are expected to obviate these issues because they are transgene-free and simple to administer as drugs. For example, because mitochondrial dysfunction causes oxidative stress by increasing the production of highly reactive free radicals such as reactive oxygen species (ROS) and reactive nitrogen species (RNS), antioxidants including MitoQ, which can reduce oxidative stress in mitochondria, have gained interests in researchers for the potential therapeutic use (Kelso et al., 2001; Smith et al., 2010). While effective, the antioxidants need to be continuously administered and cannot reverse the underlying problem by eliminating the mutant DNA. Until now, no chemical-based drugs in clinical trials have been shown to have the potential to modulate mtDNA mutations and cure mitochondrial diseases (Weissig, 2020).

Pyrrole–imidazole polyamides (PIPs) are DNA minor-groove binders composed of *N*-methylpyrrole and *N*-methylimidazole. The recognized DNA sequence can be designed with the programmed arrangement of pyrrole and imidazole: i.e., antiparallel pyrrole/pyrrole pairs recognize A/T or T/A base pairs, while imidazole/pyrrole pairs recognize G/C base pairs (Trauger et al., 1996). In 2017, we conjugated the mitochondria-penetrating peptide (MPP) known to deliver doxorubicin and chlorambucil to mitochondria (Horton et al., 2008; Chamberlain et al., 2013; Mourtada et al., 2013) with PIPs. Our PIP-MPP conjugates accumulated inside the mitochondria of live cells and their sequence-selective mtDNA binding enabled promoter-specific transcriptional control (Hidaka et al., 2017). While this method artificially alters mtDNA transcription, there is an urgent need to develop compounds that can modulate mtDNA mutations because they are associated with 80% of adult-onset mitochondrial diseases (Gorman et al., 2015).

The modular design of PIPs makes them amenable to expand their application by covalently introducing functional moieties to PIPs. For instance, PIPs have been applied in combination with DNA-alkylating reagents to specifically target oncogenic mutations in the

nuclear *KRAS* gene and were demonstrated to have antitumor effects in mouse models (Hiraoka et al., 2015). However, the bioefficacy of alkylating PIPs inside mitochondria has not been tested yet. As a proof-of-concept, here we show the synthesis, characterization and biological evaluation of a new class of multi-functional conjugate capable of sequence-specific adenine alkylation inside the mitochondria, which alters the heteroplasmy level in live cells.

RESULTS

Design and synthesis of a conjugate recognizing selective DNA sequence

The chemical structures of the compounds used in this study are shown in Figure 1A. We designed a PIP conjugated with mitochondrial penetrating peptide targeting the adjacent mtDNA sequence to m. 8950G>A point mutation. HeLa S3 cell line was previously reported to naturally have this heteroplasmic mutation (Herrnstadt et al., 2002). We then introduced chlorambucil (Chb) as a DNA-alkylating reagent to generate a multi-functional conjugate called **8950A-Chb(Cl/OH)**. Because rerouting chlorambucil, which is used as an anticancer drug, to mitochondria was known to enhance the anticancer activity, we chose chlorambucil as a suitable candidate to repurpose for the sequence-specific mtDNA alkylation and achieve our goal (Fonseca et al., 2011; Millard et al., 2013). Because PIPs position chlorambucil in the minor-groove and only adenine bases provide reactive nitrogen atoms (at the N3 position), **8950A-Chb(Cl/OH)** is expected to alkylate mutant adenine selectively (Figure 1B) (Wurtz and Dervan, 2000). As a control compound, we designed a similar PIP conjugate **Ctrl-Chb(OH/OH)** that is expected to lack binding to our target sequence (Figure 1A). To reduce nonselective alkylation of proteins, a monoalkylating chlorambucil, with one inactivated alkylating group produced via partial hydrolysis, was used (Jean et al., 2014).

Firstly, to confirm the sequence-selective DNA binding of the conjugates, the thermal stability of DNA and DNA–compound complex was analyzed by thermal melting temperature (T_m) analysis (Table 1). To prevent covalent bond formation, both alkylating groups in chlorambucil were inactivated by hydrolysis (Figure 1A, **8950A-Chb(OH/OH)** and **Ctrl-Chb(OH/OH)**). The double-stranded DNA sample was prepared with the following sequences (the binding site is underlined): 5′-d(TCCCCATACTAATTA). While no significant T_m shift was observed with **Ctrl-Chb(OH/OH)**, **8950A-Chb(OH/OH)** increased the T_m value by around 10°C, indicating that only **8950A-Chb(OH/OH)** bound to the target sequence. Despite the fact that the melting curves of the alkylation-active compounds (Figure 1A, **8950A-Chb(Cl/OH)** and **Ctrl-Chb(Cl/OH)**) showed a notable variation and T_m values calculation of the **8950A-Chb(Cl/OH)** samples was not possible, only a slight increase of T_m value (less than 5°C) was observed with **Ctrl-Chb(Cl/OH)**. This result indicates that off-target binding caused by DNA alkylation is insignificant. (Figure S2B and S2C)

Validation of sequence-specific adenine alkylation by 8950A-Chb(Cl/OH)

To examine the sequence-selectivity of DNA alkylation by **8950A-Chb(Cl/OH)**, an *in vitro* alkylation assay using capillary electrophoresis was performed (Figures 2 and S3A) (Hirose et al., 2021). The amplicon of mtDNA (ChrM: 8763–9147) was labeled with TexasRed and after alkylation reaction, the product was subjected to heat treatment to cleave the DNA at the alkylated site (Figure S3B). The resultant DNA fragments were separated by capillary electrophoresis, and the TexasRed signal chromatograms were produced (Figure 2A). While there was no difference in the alkylation pattern of the wild-type and mutant sequence alkylated by **Ctrl-Chb(Cl/OH)** (Figure 2A, left), an alkylation peak specific to the mutant sequence appeared in the samples alkylated by **8950A-Chb(Cl/OH)** (Figure 2A, right). To validate that this peak was derived from the alkylation of the target adenine, the sample was analyzed along with the Sanger sequencing sample prepared with ddATP (Figure S3C). After the manual alignment of peaks in the chromatograms to the adenine bases, the alkylation peak specific to the mutant sequence was positioned on the base before our targeted one (Figure 2B). It is important to note that the alkylation peak in the chromatograms appears one base before the actual alkylated base, because the alkylated base is removed from the DNA fragment during the sample preparation (Figure S3B). This result validates the selective alkylation of the target adenine by **8950A-Chb(Cl/OH)**. Furthermore, we newly designed **9037A-Chb(Cl/OH)** targeting adenine base at 9037 and performed an additional *in vitro* alkylation assay (Figure S4A). In accordance with our notion, **9037A-Chb(Cl/OH)** alkylated the target adenine, which supports the sequence programmability of our compounds (Figure S4B).

8950A-Chb(Cl/OH) shifts heteroplasmy level in live cells

Achieving bioefficacy in live cells is an important goal towards mitochondrial gene therapy, so we evaluated the effect of our multi-functional conjugates on the heteroplasmy level in HeLa S3 cells by quantitative PCR (qPCR). HeLa S3 cells were passaged to a new plate every 5 days, and the medium was changed 1 and 3 days after the passaging with a fresh medium containing each compound. On days 10 and 20, the treated cells were passaged to a new plate and incubated for an additional 5 days without compounds to let mtDNA recover from alkylation because alkylated mtDNA can be fragmented when the samples are heated during qPCR (the schedule of compound treatment is illustrated in Figure S5A). After total DNA extraction, the nuclear genome was digested with exonuclease V to avoid contamination of nuclear mtDNA sequences (NUMTs), which may cause experimental bias (Tobias Mourier et al., 2001). The heteroplasmy level was determined by qPCR using forward primers with

the target base at their 3′ end and a common reverse primer along with DNA polymerase possessing high discrimination ability to mismatches at the 3′-terminus (amplification refractory mutation system (ARMS)-based qPCR, Table S1 and Figures 3A and S5B) (Newton et al., 1989; Venegas and Halberg, 2012). **8950A-Chb(Cl/OH)** reduced the amount of the mutant mtDNA in a dose-dependent manner and a stable reduction was also observed from days 10 to 20. Although **Ctrl-Chb(Cl/OH)** produced slight changes in the calculated ratio at day 10 compared to the nontreated sample, the lack of further reduction at day 20 indicated that this was not a continuous effect of the conjugate. Heteroplasmy shift by **8950A-Chb(OH/OH)** was not observed, which supports the requirement of active chlorambucil (Figure 3B). Together with the data from the *in vitro* alkylation assay, this reduction in the heteroplasmy level indicates that the selective alkylation of the mutant adenine by **8950A-Chb(Cl/OH)** is effective in reducing the copy number of mutant mtDNA in live cells.

DISCUSSION

In the current study, we successfully demonstrated that a multi-functional PIP conjugate could alkylate the target adenine in a sequence-specific manner and shift the heteroplasmy level in live cells. While the mechanism of alkylated mtDNA degradation needs to be clarified, the recent shreds of evidence suggest the potential role of mitochondrial transcription factor A (TFAM). Base excision repair (BER) system that repairs deaminated and oxidized bases also repairs alkylated bases (Fu et al., 2020). During BER, abasic (AP) sites with high chemical reactivity are generated, and BER and mtDNA degradation are the major pathways to deal with AP sites (Kozhukhar et al., 2016). Recently, TFAM was reported to promote degradation of mtDNA containing AP sites by inducing single-strand breaks and DNA-TFAM cross-links. Accordingly, the TFAM-mediated pathway is expected to eliminate the mtDNA alkylated by our compounds (Xu et al., 2019). Our proof-of-concept study provides a new chemical approach to develop conjugates for the gene therapy of mitochondrial diseases, which has only been demonstrated with biological tools so far.

Our current approach requires amplification of wild-type mtDNA along with the removal of mutant mtDNA and cannot be applied to homoplasmic mtDNA mutations where no wild-type mtDNA is available. However, mitochondrial base “editing” technology has been reported recently to target such mutations by using cytidine deaminase, which corrects mutated C-G base pairs into T-A base pairs (Mok et al., 2020). The development of a similar system to target homoplasmic mutations needs to be explored to overcome this current bottleneck.

SIGNIFICANCE

Mitochondrial DNA mutations are difficult to target and until now, there are no small molecule drug conjugates available capable of eliminating mutated mitochondrial DNA inside live cells. Previously, peptide nucleic acid (PNA) oligomers targeting mtDNA mutations were applied to replication inhibition of mutant mtDNA. Although conjugation of PNA oligomers with mitochondrial-targeting peptides or triphenylphosphonium cation-enhanced mitochondrial delivery of PNA oligomers, their activity has only been demonstrated in *in vitro* systems and an artificial heteroplasmy shift in live cells has not been achieved (Chinnery et al., 1999; Flierl et al., 2003; Muratovska et al., 2001; Taylor et al., 1997). Here, we successfully demonstrated that our multi-functional PIP conjugate shifts the heteroplasmy level in live cells by alkylating the target mutation. The major advantage of our multi-functional conjugates is that we can preprogram them to recognize specific DNA sequences by rearranging the combination of pyrrole and imidazole rings. This proof-of-concept study targeting a nonpathogenic mutation (m. 8950G>A) in HeLa S3 cells can be extended to the point mutations generating adenine (or thymine) ensuing several mitochondrial diseases including Leber's hereditary optic neuropathy (m.11778G>A and m.3460G>A) and MELAS syndrome (m.3697G>A and m.13513G>A) (Wallace et al., 1988; Huoponen et al., 1991; Kirby et al., 2004; Santorelli et al., 1997). Modulation of the pathogenic mtDNA mutations will be addressed in future studies to advance their application as therapeutic tools for mitochondrial diseases. Nevertheless, our multi-functional conjugate could open new vistas of opportunities to drug the undruggable mutations inside live cells.

ACKOWLEDGMENTS

Capillary electrophoresis was performed at the Medical Research Support Center, Graduate School of Medicine, Kyoto University. We thank JCRB cell bank for providing HeLa cells (JCRB9004). This work was supported by AMED [JP20am0101101 (Platform Project for Supporting Drug Discovery and Life Science Research (BINDS) to H.S.)], JSPS [18J21755 (Grant-in-Aid for JSPS Fellows) to T. H., 19H03349 (Grants-in-Aid for Scientific Research (B)) to G.N.P, and 16H06356 (Grants-in-Aid for Scientific Research (S)) to H.S.], Takeda Science Foundation (to G.N.P.), Hirose Foundation (to G.N.P.) and NIH awards R01CA236350 (to H.S.).

AUTHOR CONTRIBUTION

Conceptualization, T.H., G.N.P., and H.S.; Organic synthesis, T.H., K.H., and T.B.; in vitro and cell assays, T.H.; Writing – Original Draft, T.H.; Writing – Review & Editing, G.N.P, and H.S.; Supervision, G.N.P. and H.S.

DECLARATION OF INTETERESTS

The authors declare no competing interests.

REFERENCES

Bacman, S.R., Williams, S.L., Pinto, M., Peralta, S., Moraes, C.T. (2013). Specific elimination of mutant mitochondrial genomes in patient-derived cells by mitoTALENs. Nat. Med. 19, 1111-1113.

Bacman, S.R., Kauppila, J.H.K., Pereira, C.V., Nissanka, N., Miranda, M., Pinto, M., Williams, S.L., Larsson, N.G., Stewart, J.B., Moraes, C.T. (2018). MitoTALEN reduces mutant mtDNA load and restores tRNA(Ala) levels in a mouse model of heteroplasmic mtDNA mutation. Nat. Med. 24, 1696-1700.

Baird, E.E., Dervan, P.B. (1996) Solid Phase Synthesis of Polyamides Containing Imidazole and Pyrrole Amino Acids. L. Am. Chem. Soc. 118, 6141-6146.

Bayona-Bafaluy, M. P., Blits, B., Battersby, B. J., Shoubridge, E. A., Moraes, C. T. (2005). Rapid directional shift of mitochondrial DNA heteroplasmy in animal tissues by a mitochondrially targeted restriction endonuclease. Proc. Natl. Acad. Sci. U.S.A. 102, 14392-14397.

Boulet, L., Karpati, G., and Shoubridge, E.A. (1992). Distribution and threshold expression of the tRNA(Lys) mutation in skeletal-muscle of patients with myoclonic epilepsy and ragged-red fibers (MERRF). Am. J. Hum. Genet. 51, 1187-1200.

Chamberlain, G.R., Tulumello, D.V., and Kelley, S.O. (2013). Targeted Delivery of Doxorubicin to Mitochondria. ACS Chem. Biol. 8, 1389-1395.

Chinnery, P.F., Taylor, R.W., Diekert, K., Lill, R., Turnbull, D.M., and Lightowlers, R.N. (1999). Peptide nucleic acid delivery to human mitochondria. Gene Ther. 6, 1919-1928.

Flierl, A., Jackson, C., Cottrell, B., Murdock, D., Seibel, P., and Wallace, D.C. (2003). Targeted delivery of DNA to the mitochondrial compartment via import sequence-conjugated peptide nucleic acid. Mol. Ther. 7, 550-557.

Fonseca, S.B., Pereira, M.P., Mourtada, R., Gronda, M., Horton, K.L., Hurren, R., Minden, M.D., Schimmer, A.D., and Kelley, S.O. (2011). Rerouting Chlorambucil to Mitochondria Combats Drug Deactivation and Resistance in Cancer Cells. Chem. Biol. 18, 445-453.

Fu, Y., Tigano, M., and Sfeir, A. (2020). Safeguarding mitochondrial genomes in higher eukaryotes. Nat. Struct. Mol. Biol. 27, 687-695.

Gammage, P. A., Rorbach, J., Vincent, A. I., Rebar, E. J., Minczuk, M. (2014). Mitochondrially targeted ZFNs for selective degradation of pathogenic mitochondrial genomes bearing large-scale deletions or point mutations. EMBO Mol. Med. 6, 458-466.

Gammage, P.A., Viscomi, C., Simard, M.L., Costa, A.S.H., Gaude, E., Powell, C.A., Van Haute, L., McCann, B., Rebelo-Guiomar, P., Cerutti, R., Zhang, L., Rebar, E.J., Zeviani, M., Frezza, C., Stewart, J.B., Minczuk, M. (2018). Genome editing in mitochondria corrects a pathogenic mtDNA mutation in vivo. Nat. Med. 24, 1691-1695.

Gorman, G.S., Chinnery, P.F., DiMauro, S., Hirano, M., Koga, Y., McFarland, R., Suomalainen, A., Thorburn, D.R., Zeviani, M., and Turnbull, D.M. (2016). Mitochondrial diseases. Nat. Rev. Dis. Primers 2, 16080.

Gorman, G.S., Schaefer, A.M., Ng, Y., Gomez, N., Blakely, E.L., Alston, C.L., Feeney, C., Horvath, R., Yu-Wai-Man, P., Chinnery, P.F., Taylor, R.W., Turnbull, D.M., McFarland, R., (2015). Prevalence of Nuclear and Mitochondrial DNA Mutations Related to Adult Mitochondrial Disease. Ann. Neurol. 77, 753-759.

Herrnstadt, C., Preston, G., Andrews, R., Chinnery, P., Lightowlers, R.N., Turnbull, D.M., Kubacka, I., and Howell, N. (2002). A high frequency of mtDNA polymorphisms in HeLa cell sublines. Mutat. Res. 501, 19-28.

Hidaka, T., Pandian, G.N., Taniguchi, J., Nobeyama, T., Hashiya, K., Bando, T., and Sugiyama, H. (2017). Creation of a Synthetic Ligand for Mitochondrial DNA Sequence Recognition and Promoter-Specific Transcription Suppression. J. Am. Chem. Soc. 139, 8444-8447.

Hiraoka, K., Inoue, T., Taylor, R.D., Watanabe, T., Koshikawa, N., Yoda, H., Shinohara, K., Takatori, A., Sugimoto, H., Maru, Y., et al. (2015). Inhibition of KRAS codon 12 mutants using a novel DNA-alkylating pyrrole-imidazole polyamide conjugate. Nat. Commun. 6, 6706.

Hirose, Y., Hashiya, K., Bando, T., and Sugiyama, H. (2021) Evaluation of the DNA Alkylation Property of a Chlorambucil Conjugated Cyclic Pyrrole-Imidazole Polyamide. Chem. Eur. J. 27, 2782-2788.

Holt, I.J., Harding, A.E., and Morganhughes, J.A. (1988). Deletions of muscle mitochondrial-DNA in patients with mitochondrial myopathies. Nature 331, 717-719.

Hopper, R.K., Carroll, S., Aponte, A.M., Johnson, D.T., French, S., Shen, R.F., Witzmann, F.A., Harris, R.A., and Balaban, R.S. (2006). Mitochondrial matrix phosphoproteome: Effect of extra mitochondrial calcium. Biochemistry 45, 2524-2536.

Horton, K.L., Stewart, K.M., Fonseca, S.B., Guo, Q., and Kelley, S.O. (2008). Mitochondria-penetrating peptides. Chem. Biol. 15, 375-382.

Hughes, D.A., Jastroch, M., Stoneking, M., and Klingenspor, M. (2009). Molecular evolution of UCP1 and the evolutionary history of mammalian non-shivering thermogenesis. BMC Evol. Biol. 9, 4.

Huoponen, K., Vilkki, J., Aula, P., Nikoskelainen, E.K., and Savontaus, M.-L. (1991). A new mtDNA mutation associated with Leber hereditary optic neuroretinopathy. Am. J. Hum. Genet. 48, 1147-1153.

Jackson, C.B., Turnbull, D.M., Minczuk, M., and Gammage, P.A. (2020). Therapeutic Manipulation of mtDNA Heteroplasmy: A Shifting Perspective. Trends Mol. Med. 26, 698-709.

Jean, S.R., Pereira, M.P., and Kelley, S.O. (2014). Structural Modifications of Mitochondria-Targeted Chlorambucil Alter Cell Death Mechanism but Preserve MDR Evasion. Mol. Pharm. 11, 2675-2682.

Kirby, D.M., McFarland, R., Ohtake, A., Dunning, C., Ryan, M.T., Wilson, C., Ketteridge, D., Turnbull, D.M., Thorburn, D.R., and Taylor, R.W. (2004). Mutations of the mitochondrial ND1 gene as a cause of MELAS. J. Med. Genet. 41, 784-789.

Kelso, G.F., Porteous, C.M., Coulter, C.V., Hughes, G., Porteous, W.K., Ledgerwood, E.C., Smith, R. A., Murphy, M. P. (2001). Selective targeting of a redox-active ubiquinone to mitochondria within cells: antioxidant and antiapoptotic properties. J. Biol. Chem. 276, 4588-4596.

Kogelnik, A.M., Lott, M.T., Brown, M.D., Navathe, S.B., and Wallace, D.C. (1996). MITOMAP: A human mitochondrial genome database. Nucleic Acids Res. 24, 177-179.

Kozhukhar, N., Spadafora, D., Fayzulin, R., Shokolenko, I.N., and Alexeyev, M. (2016). The efficiency of the translesion synthesis across abasic sites by mitochondrial DNA polymerase is low in mitochondria of 3T3 cells. Mitochondrial DNA A DNA Mapp. Seq. Anal. 27, 4390-4396.

Millard, M., Gallagher, J.D., Olenyuk, B.Z., and Neamati, N. (2013). A selective mitochondrial-targeted chlorambucil with remarkable cytotoxicity in breast and pancreatic cancers. J. Med. Chem. 56, 9170-9179.

Minoshima, M., Bando, T., Sasaki, S., Fujimoto, J., and Sugiyama, H. (2008). Pyrrole-imidazole hairpin polyamides with high affinity at 5'–CGCG–3' DNA sequence; influence of cytosine methylation on binding. Nucleic Acids Res. 36, 2889-2894.

Mok, B.Y., Moraes, M.H., Zeng, J., Bosch, D.E., Kotrys, A.V., Raguram, A., Hsu, F., Radey, M.C., Peterson S.B., Mootha, V.K., Mougous, J.D., Liu D.R. (2020). A bacterial cytidine deaminase toxin enables CRISPR-free mitochondrial base editing. Nature 583, 631-637.

Mourier, T., Hansen, A.J., Willerslev, E., and Arctander, P. (2001). The Human Genome Project Reveals a Continuous Transfer of Large Mitochondrial Fragments to the Nucleus. Mol. Biol. Evol. 18, 1833-1837.

Mourtadal, R., Fonsecal, S.B., Wisnovsky, S.P., Pereira, M.P., Wang, X., Hurren, R., Parfitt, J., Larsen, L., Smith, R. A. J., Murphy, M.P., Schimmer, A.D., Kelley, S.O. (2013). Re-Directing an Alkylating Agent to Mitochondria Alters Drug Target and Cell Death Mechanism. PLoS One 8, e60253.

Muratovska, A., Lightowlers, R.N., Taylor, R.W., Turnbull, D.M., Smith, R.A.J., Wilce, J.A., Martin, S.W., and Murphy, M.P. (2001). Targeting peptide nucleic acid (PNA) oligomers to mitochondria within cells by conjugation to lipophilic cations: implications for mitochondrial DNA replication, expression and disease. Nucleic Acids Res. 29, 1852-1863.

Newton, C.R., Graham, A., Heptinstall, L.E., Powell, S.J., Summers, C., Kalsheker, N., Smith, J.C., and Markham, A.F. (1989). Analysis of any point mutation in DNA. The amplification refractory mutation system (ARMS). Nucleic Acids Res. 17, 2503-2516.

Rasola, A., and Bernardi, P. (2011). Mitochondrial permeability transition in Ca2+-dependent apoptosis and necrosis. Cell Calcium 50, 222-233.

Rizzuto, R., De Stefani, D., Raffaello, A., and Mammucari, C. (2012). Mitochondria as sensors and regulators of calcium signalling. Nat. Rev. Mol. Cell Biol. 13, 566-578.

Robin, E.D., and Wong, R. (1988). Mitochondrial-DNA molecules and virtual number of mitochondria per cell in mammalian-cells. J. Cell. Physiol. 136, 507-513.

Santorelli, F.M., Tanji, K., Kulikova, R., Shanske, S., Vilarinho, L., Hays, A.P., and DiMauro, S. (1997). Identification of a novel mutation in the mtDNA ND5 gene associated with MELAS. Biochem. Biophys. Res. Commun. 238, 326-328.

Sawatani, Y., Kashiwazaki, G., Chandran, A., Asamitsu, S., Guo, C., Sato, S., Hashiya, K., Bando, T., Sugiyama, H. (2016). Sequence-specific DNA binding by long hairpin pyrrole-imidazole polyamides containing an 8-amino-3, 6-dioxaoctanoic acid unit. Bioorg. Med. Chem. 24, 3603-3611.

Smith, R.A.J. and Murphy, M.P. (2010). Animal and human studies with the mitochondria-targeted antioxidant MitoQ. Ann. N. Y. Acad. Sci. 1201, 96-103.

Spinelli, J.B., and Haigis, M.C. (2018). The multifaceted contributions of mitochondria to cellular metabolism. Nat. Cell Biol. 20, 745-754.

Syed, J., Pandian, G.N., Sato, S., Taniguchi, J., Chandran, A, Hashiya, K., Bando, T., Sugiyama, H. (2014) Targeted suppression of EVI1 oncogene expression by sequence-specific pyrrole-imidazole polyamide. Chem. Biol. 21, 1370-1380.

Taylor, R.W., Chinnery, P.F., Turnbull, D.M., and Lightowlers, R.N. (1997). Selective inhibition of mutant human mitochondrial DNA replication in vitro by peptide nucleic acids. Nat. Genet. 15, 212-215.

Trauger, J.W., Baird, E.E., and Dervan, P.B. (1996). Recognition of DNA by designed ligands at subnanomolar concentrations. Nature 382, 559-561.

Venegas, V., and Halberg, M.C. (2012). Quantification of mtDNA mutation heteroplasmy (ARMS qPCR). Methods Mol Biol 837, 313-326.

Wallace, D.C., Singh, G., Lott, M.T., Hodge, J.A., Schurr, T.G., Lezza, A.M.S., Elsas, L.J., and Nikoskelainen, E.K. (1988). Mitochondrial DNA Mutation Associated with Leber's Hereditary Optic Neuropathy. Science 242, 1427-1430.

Weissig, V. (2020). Drug Development for the Therapy of Mitochondrial Diseases. Trends Mol. Med. 26, 40-57.

Wurtz, N.R., and Dervan, P.B. (2000). Sequence specific alkylation of DNA by hairpin pyrrole–imidazole polyamide conjugates. Chem. Biol. 7, 153-161.

Xu, W., Boyd, R.M., Tree, M.O., Samkari, F., and Zhao, L. (2019). Mitochondrial transcription factor A promotes DNA strand cleavage at abasic sites. Proc. Natl. Acad. Sci. U. S. A. 116, 17792-17799.

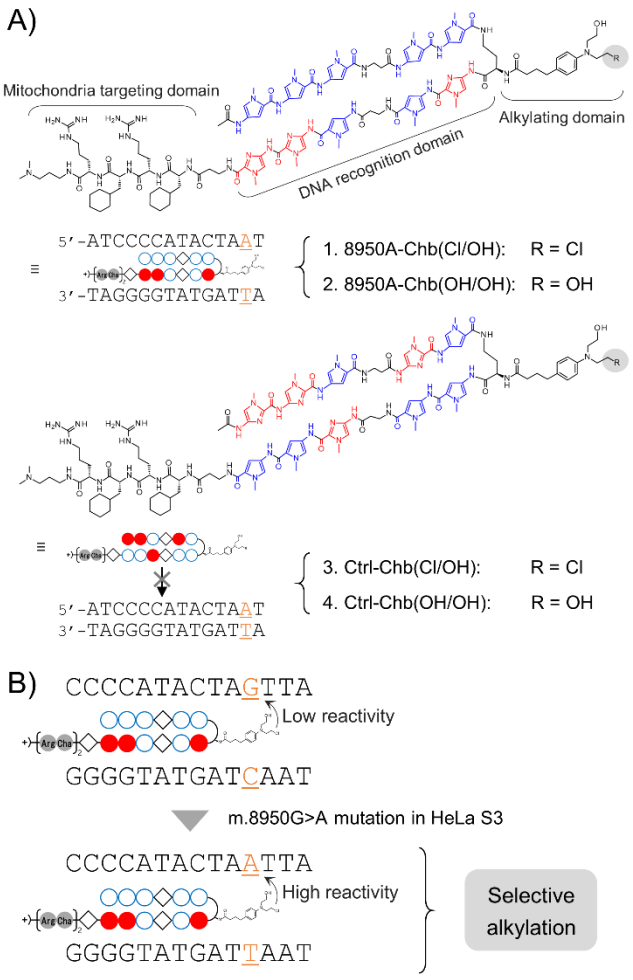

Figure 1. (A) The chemical structure of the multi-functional conjugates used in this study. The characterization data are shown in Figure S1. The target point mutation is shown in orange. (B) Mechanism of mutation-specific DNA alkylation in HeLa S3 cells by **8950A-Chb(Cl/OH)**.

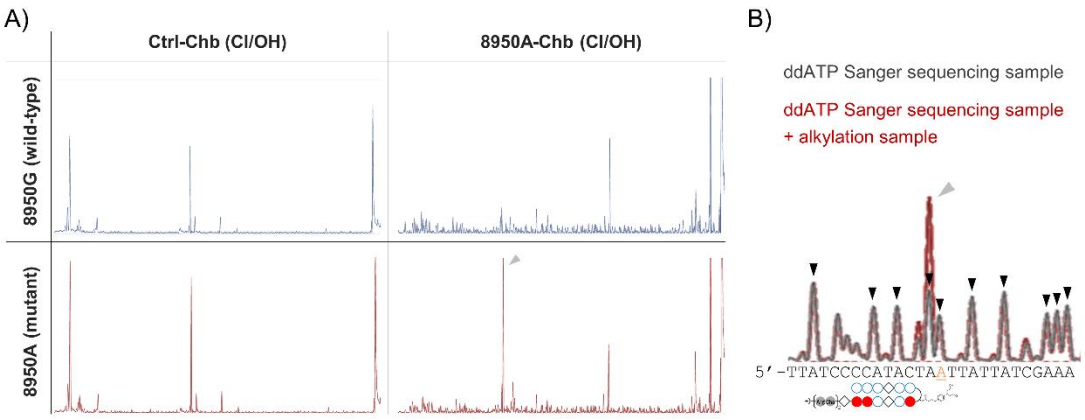

Figure 2. The *in vitro* alkylation assay by capillary electrophoresis. (A) Chromatograms from the capillary electrophoresis of DNA sequences (with and without m.8950G>A mutation) alkylated with **Ctrl-Chb(Cl/OH)** and **8950A-Chb(Cl/OH)**. (B) Determination of the alkylated base specific to the mutant sequence alkylated by **8950A-Chb(Cl/OH)**. The peaks assigned to adenine bases are indicated with black arrows, and the alkylation peak is indicated with a gray arrow. The target adenine is shown in orange.

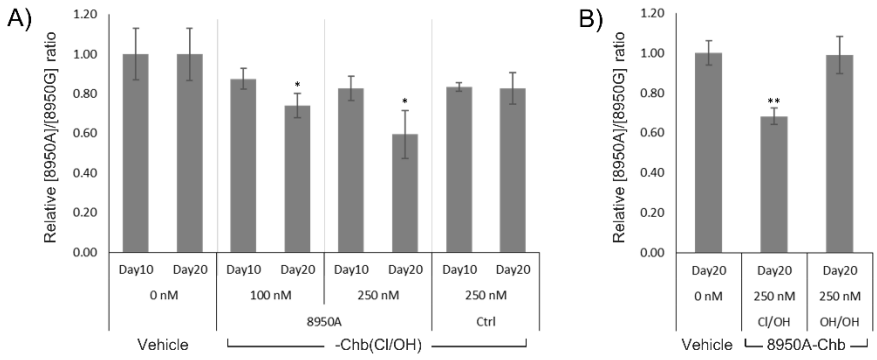

Figure 3. Shift of heteroplasmy level in HeLa S3 cells after incubation with (A) **8950A-Chb(Cl/OH)** and **Ctrl-Chb(Cl/OH)**, and (B) **8950A-Chb(Cl/OH)** and **8950A-Chb (OH/OH)**. The relative ratio of mutant ([8950A]) to wild-type ([8950G]) mtDNA was determined by quantitative PCR. Each value is normalized to the mean of vehicle control containing the same concentration of DMSO as other samples (final concentration: 0.1%) at corresponding time points. Each bar represents the mean ±SD (n = 3) and statical significance was determined by the Student t-test: $*P < 0.05$, $**P < 0.01$.

Table 1. Shift of T_m values by **8950A-Chb(OH/OH)** and **Ctrl-Chb(OH/OH)**. The average T_m values were calculated from three melting temperature analyses and each standard deviation is indicated in parentheses. ΔT_m = T_m (DNA–compound complex) – T_m (DNA). Representative melting curves are shown in Figure S2A.

DNA only	+ **8950A-Chb(OH/OH)**		+ **Ctrl-Chb(OH/OH)**	
T_m /°C	T_m /°C	ΔT_m /°C	T_m /°C	ΔT_m /°C
34.24 (± 0.28)	44.20 (± 0.06)	9.97	34.75 (± 0.33)	0.52

STAR METHODS

RESOURCE AVAILABILITY

Lead contact

Further information and requests for resources and reagents should be directed to and will be fulfilled by the lead contact, Hiroshi Sugiyama (hs@kuchem.kyoto-u.ac.jp).

Materials availability

Plasmids, DNA fragments, compounds generated in this study will be made available upon reasonable request.

Data and code availability

Data generated in this study will be made available upon reasonable request.

EXPERIMENTAL MODEL AND SUBJECT DETAILS

Cell lines

HeLa (JCRB9004) and HeLa S3 cells were purchased from JCRB Cell Bank (Japan) and ATCC, respectively. All cells were maintained in Dulbecco's Modified Eagle Medium (ThermoFisher Scientific) supplemented with 10 % fetal bovine serum (FBS, Sigma) in a humidified CO_2 incubator at 37°C.

METHOD DETAILS

General information of synthesis

The reagents were purchased from standard suppliers. The solid-phase synthesis was performed using an automated synthesizer, PSSM-8 (Shimadzu), with a computer-assisted operation system. Analytical reversed-phase high-performance liquid chromatography (HPLC) was performed on a JASCO HPLC system (JASCO Engineering UV2075 UV/vis detector and a PU-2089 plus gradient pump) equipped with Chemcobond 5-ODS-H reversed-phase column (4.6×150 mm). H_2O (+0.1% trifluoroacetic acid) and acetonitrile were used as the mobile phase, and the program was a linear gradient of 0 to 100% acetonitrile in 20 or 40 min at a flow rate of 1.0 mL/min. Absorbance at 254 nm was monitored. MALDI-TOF mass spectroscopy was performed with the Microflex system (Bruker).

Solid-phase synthesis of pyrrole-imidazole polyamides and chlorambucil conjugation

Each Fmoc monomer units (Fmoc-D-Arg(Pbf)-OH, Fmoc-cyclohexylalanine-OH, Fmoc-β-alanine-OH, Fmoc-Dab(Boc)-OH, Fmoc-*N*-methylpyrrole(Py)-OH and Fmoc-*N*-methylimidazole(Im)-OH) was introduced sequentially to Fmoc-D-Arg(Pbf)-Alko resin

using an automated synthesizer, PSSM-8 (Shimadzu). To overcome the difficulty of coupling Py after Im, Fmoc-Py-Im-OH dimer unit was also used to improve synthesis efficiency (Baird et al., 1996; Minoshima et al., 2008). Each coupling reaction was performed at room temperature for one hour in *N*-Methyl-2-pyrrolidone (NMP) containing 4 eq of HCTU, *N*, *N*-diisopropylethylamine (DIEA) and each Fmoc monomer unit, followed by Fmoc deprotection in 20% piperidine in *N*, *N*-dimethylformamide (DMF). After the solid-phase synthesis, the resin was incubated with 20% acetic anhydride in DMF at room temperature to cap the N-terminal with an acetyl group. Synthesized compounds were cleaved with *N*, *N*-dimethylaminopropylamine at 55°C for 3 hours. The reaction solution was drained into ether, and the resulting solid was dried *in vacuo*.

Before coupling reaction with chlorambucil, the Boc group of the turn unit (Dab) was removed with a deprotection cocktail (trifluoroacetic acid: dichloromethane (30:70 v/v%)) at room temperature for 5 minutes. The reaction solution was drained into the ether, and the resulting solid was dried *in vacuo*.

After Boc deprotection, the compounds were coupled with chlorambucil in DMF by adding 2-4 eq of chlorambucil, 3-6 eq of 1-[Bis(dimethylamino)methylene]-1*H*-benzotriazolium 3-Oxide Hexafluorophosphate (HBTU) and 4-8 eq of *N*, *N*-diisopropylethylamine (DIPEA) and shaking at room temperature for 3.5 hours to overnight. The reaction solution was drained into ether, and the resulting solid was dried *in vacuo*.

After chlorambucil coupling, the protecting groups of arginine residues (Pbf groups) were removed with a deprotection cocktail (trifluoroacetic acid: triisopropylsilane: water (95:2.5:2.5 v/v%)) at room temperature for 30 minutes. The reaction solution was drained into ether, and the resulting solid was dried *in vacuo*, obtaining **8950A-Chb(Cl/Cl)**, **9037A-Chb(Cl/Cl)** and **Ctrl-Chb(Cl/Cl)**.

Synthesis of 8950A-Chb(Cl/OH)

After Pbf deprotection, 11.2 mg of **8950A-Chb(Cl/Cl)** was hydrolyzed in acetonitrile/water (+0.1% trifluoroacetic acid) (300 μL and 750 μL, respectively) at 50°C for 1 hour 15 min and purified by reversed-phase HPLC using a JASCO HPLC system (JASCO Engineering UV2075 UV/vis detector and a PU-2089 plus gradient pump) with a preparative C_{18} (ODS) column (COSMOSIL 5C_{18}-MS-II, 10ID x 150 mm). Deionized water (+0.1% trifluoroacetic acid) and acetonitrile were used as the mobile phase. HPLC and MALDI-TOF mass spectroscopy was performed for the characterization of the purified compounds. The characterization data is shown in Figure S1.

Synthesis of Ctrl-Chb(Cl/OH)

4.1 mg of **Ctrl-Chb(Cl/Cl)** was hydrolyzed in acetonitrile/ water (+0.1% trifluoroacetic acid) (200 μL each) at 55°C for 2 hours. Purification and characterization were performed as explained above, and the characterization data is shown in Figure S1.

Synthesis of 9037A-Chb(Cl/OH)

8.0 mg of **9037A-Chb(Cl/Cl)** was hydrolyzed in acetonitrile/ water (+0.1% trifluoroacetic acid) (300 μL and 750 μL, respectively) at 45°C for 2 hours. Purification and characterization were performed as explained above, and the characterization data is shown in Figure S1.

Synthesis of 8950A-Chb(OH/OH) and Ctrl-Chb(OH/OH)

6.2 mg of **8950A-Chb(Cl/Cl)** and 4.7 mg of **Ctrl-Chb(Cl/Cl)** were hydrolyzed in acetonitrile/ water (+0.1% trifluoroacetic acid) (300 μL each) at 55°C overnight. Purification and characterization were performed as explained above, and the characterization data is shown in Figure S1.

Preparation of DMSO solution of each compound

The powder of each compound was dissolved in DMSO, and the concentration was determined from the calculation formula below using the maximum absorbance in 300-310 nm measured by a Nanodrop ND-1000 (ThermoFisher Scientific):

$$\mathrm{c} = \frac{Abs}{9900 \times a \times d} \quad (M)$$

(a: total number of pyrrole and imidazole rings, d (cm): optical path length (0.1 cm for Nanodrop ND-1000), Abs = Maximum absorbance in 300-310 nm)

T_m analysis

The buffer for T_m analysis was an aqueous solution of 10 mM sodium chloride and 10 mM sodium cacodylate at pH 7.0 containing 2.5 v/v% DMSO. The concentration of polyamides and dsDNA was 5 and 2.5 mM, respectively (2:1 stoichiometry). Before the analyses, the samples were annealed from 65°C to 5°C at 1.0°C/min. Absorbance at 260 nm was recorded from 5°C to 65°C at a rate of 1.0°C/min using a spectrophotometer V-650 (JASCO) with a thermocontrolled PAC-743R cell changer (JASCO) and a thermal circulator F25-ED (Julabo).

Alkylation assay by capillary electrophoresis

Cloning of mtDNA sequence (ChrM: 8763-9333) into pGEM-T-easy vector

mtDNA was prepared from HeLa cells by total DNA extraction using QIAamp DNA mini

kit (QIAGEN), nuclear DNA digestion with exonuclease V (New England Biolabs), and clean-up with AMPure XP beads (Beckman Coulter) following the manufacture's protocol. The mtDNA sequence (ChrM: 8763-9333) was amplified by PCR from the extracted mtDNA using GoTaq® Green Master Mix (Promega) and PCR primers (forward primer: 5'-TGCCACAACTAACCTCCTCG, reverse primer: 5'- GGAGCGTTATGGAGTGGAAGT). After PCR clean-up with Wizard® SV Gel and PCR Clean-Up System (Promega), the PCR product was ligated with pGEM®-T Easy Vector (Promega) using Ligation high Ver.2 (Toyobo). The ligation sample was transformed into Competent high JM109 cells (Toyobo) and subjected to single-cell cloning and amplification (pGEM-8950G).

Introduction of m.8950G>A point mutation into the cloned sequence

The m.8950G>A point mutation was introduced into the cloned sequence by invert PCR using KOD -Plus- Mutagenesis Kit (Toyobo) with PCR primers possessing the target point mutation (forward primer: 5'-ATTATTATCGAAACCATCAGCCTACTCATTCAAC, reverse primer: 5'-TAGTATGGGGATAAGGGGTGTAGGTG, the target point mutation is underlined). The invert PCR and successive *DpnI* digestion and ligation reaction were performed following the manufacture's protocol. The ligation sample was transformed into ECOS JM109 cells (Nippon Gene) and subjected to single-cell cloning and amplification (pGEM-8950A).

Sequencing of the cloned mtDNA sequence

The mtDNA sequence (ChrM: 8763-9333) with and without the m.8950G>A point mutation introduced into the pGEM-T-easy vector was confirmed by DNA sequencing. Sequencing reactions were performed in a BioRad DNA Engine Dyad PTC-220 Peltier Thermal Cycler using ABI PRISM® BigDye® Terminator v3.1 Cycle Sequencing Kits (Applied Biosystems), following the protocols supplied by the manufacturer. Single-pass sequencing was performed on each template using the same primers used for the PCR amplification of the mtDNA sequence. The fluorescent-labeled fragments were purified from the unincorporated terminators with an ethanol precipitation protocol. The samples were resuspended in distilled water and subjected to electrophoresis in an ABI 3730xl sequencer (Applied Biosystems).

Preparation of non-labeled and TexasRed-labeled template DNA

The mtDNA sequence (ChrM: 8763-9147) with and without the m.8950G>A point mutation in the pGEM-T-easy vector was subjected to PCR amplification using GoTaq® Green Master Mix (Promega) with non-labeled (5'-TGCCACAACTAACCTCCTCG) or

TexasRed-labeled forward primers (5'- TexasRed-TGCCACAACTAACCTCCTCG) and non-labeled reverse primer (5'-GGCGACAGCGATTTCTAGGATAG). The PCR product was purified using Wizard® SV Gel and PCR Clean-Up System (Promega) to obtain non-labeled and TexasRed-labeled template DNA.

*Alkylation of TexasRed-labeled mtDNA fragments by **8950A-Chb (Cl/OH)** and **Ctrl-Chb (Cl/OH)***

The labeled template DNA with and without the m.8950G>A point mutation (200 nM) was mixed with each compound (800 nM) in sodium phosphate buffer (50 mM, pH7) containing 10% DMSO and incubated at 37°C for 20 hours. After the alkylation reaction, the samples were heated at 95°C for 5 minutes to remove alkylated bases and cleave the DNA strand, and the residual sugar moiety was removed by further incubation at 95°C for 25 minutes in the presence of 1 M of piperidine (Figure S3 B). The fragmented samples were purified using Performa® DTR Gel Filtration Cartridges (Edge Biosystems) and lyophilized. The terminal phosphate group was removed by phosphatase treatment (New England Biolabs), and the samples were purified again using Performa® DTR Gel Filtration Cartridges (Edge Biosystems) (Figure S3 B). The samples were lyophilized and dissolved in Hi-Di™ Formamide (Applied Biosystems) and subjected to capillary electrophoresis.

Preparation of Sanger sequencing sample with dideoxyATP (ddATP)

The Sanger sequencing sample was prepared by Thermo Sequenase Cycle Sequencing Kit (Applied Biosystems) (Figure S3 C). The non-labeled template DNA (ChrM: 8763-9147) with the m.8950G>A point mutation was mixed with the TexasRed-labeled primer (5'-TexasRed-TGCCACAACTAACCTCCTCG) and Thermo Sequenase DNA polymerase in the reaction buffer, and the mixture was added to ddATP termination mix containing 150 μM of each dNTPs and 1 μM of ddATP. The amplification reaction was performed with the following thermocycling condition: 95°C, 3 min > [95°C, 30 sec > 60°C, 30 sec > 72°C, 1 min] (40 cycles) > 72°C, 5 min > 12°C. The TexasRed-labeled fragments were purified using Performa® DTR Gel Filtration Cartridges (Edge Biosystems) and lyophilized. The dried samples were dissolved in Hi-Di™ Formamide (Applied Biosystems) and subjected to capillary electrophoresis.

Capillary electrophoresis

The samples dissolved in Hi-Di™ Formamide (Applied Biosystems) were subjected to capillary electrophoresis in a 3500xl Genetic Analyzer (Applied Biosystems). The chromatograms of TexasRed signal saved in ab1 format were visualized in DNA Baser

Assembler software (Heracle BioSoft S.R.L.) and exported as bitmap images.

To determine the alkylated base, the chromatogram of a mixture of the alkylation sample and the Sanger sequencing sample was compared with that of the only Sanger sequencing sample. Both chromatograms were manually aligned, and each peak was assigned to adenine bases in the DNA sequence.

Compound treatment and quantitative PCR (qPCR) analysis

HeLa S3 cells were seeded on a 24-well plate at 1×10^4 cells/ well one day before the treatment. The cells were passaged to a new 24-well plate in a growth medium every five days, and the medium was changed one and three days after the passaging with OPTI-MEM medium (ThermoFisher Scientific) supplemented with 2% FBS, 0.1% DMSO and each compound. On day 10 and 20, the cells were passaged to a 12-well plate at 2×10^4 cells/ well in growth medium (without the compounds) and incubated for five days for recovery from DNA alkylation (Figure S5 A).

After the recovery period, total DNA was extracted by the QIAamp DNA mini kit (Qiagen). The extracted DNA (1 mg) was digested with exonuclease V (New England Biolabs) to remove genomic DNA and purified again with QIAquick PCR Purification Kit (Qiagen). The obtained mtDNA was diluted to 5 ng/mL with nuclease-free water.

PCR reaction mixture was prepared with the HiDi® 2x PCR Master Mix (myPOLS Biotec.) and GreenDye 20x (myPOLS Biotec.), and the qPCR reaction was performed and monitored on LightCycler 480 System II (Roche). The primer sequences used in this experiment are listed in Table S1.

QUANTIFICATION AND STATISTICAL ANALYSIS

For T_m analyses, T_m values were calculated from melting curves with Spectra Manager software (JASCO) by using 2nd derivative method. The average T_m values and standard deviations were calculated from three T_m analyses.

In quantitative PCR experiments, Cp values were calculated from amplification curves using LightCycler® 480 Software, Version 1.5 (Roche), and the relative amount of mutant mtDNA ([8950A]) to wild-type mtDNA ([8950G]) was calculated from the averaged Cp values of three replicates of each sample. The calculated ratio was normalized to the mean value of non-treated samples. Statistical analysis was performed using a Student's unpaired two-tailed t-test.